

A Catalytic and Positively Thermosensitive Molecularly Imprinted Polymer

Songjun Li, Yi Ge,* and Anthony P. F. Turner*

A catalytic and positively thermosensitive molecularly imprinted polymer is reported. This unique imprinted polymer was composed of 4-nitrophenyl phosphate-imprinted networks that exhibited a thermosensitive interpolymer interaction between poly(2-trifluoromethylacrylic acid) (PTFMA) and poly(1-vinylimidazole) (PVI), which contains catalytically active sites. At a relatively low temperature (such as 20 °C), this imprinted polymer did not demonstrate significant catalytic activity for the hydrolysis of 4-nitrophenyl acetate due to the interpolymer complexation between PVI and PTFMA, which blocked access to the active sites of PVI and caused shrinking of the polymer. Conversely, at higher temperatures (such as 40 °C), this polymer showed significant catalytic activity resulting from the dissociation of the interpolymer complexes between PVI and PTFMA, which facilitated access to the active sites of PVI and inflated the polymer. Unlike previously reported poly(*N*-isopropylacrylamide)-based molecularly imprinted polymers, which demonstrated decreased molecular recognition and catalytic activity with increased temperatures, i.e., negatively thermosensitive molecular recognition and catalysis abilities, this imprinted polymer exploits the unique interpolymer interaction between PVI and PTFMA, enabling the reversed thermal responsiveness.

highly specific molecular recognition and catalysis. Significant applications of molecular imprinting include separations,^[4,5] solid phase extraction,^[6] adsorption,^[7] catalysis,^[8] and sensing.^[9] During the molecular imprinting process, the template and functional monomers are first allowed to form a self-assembled architecture where the functional monomers are regularly positioned around the template. Polymerization is then performed to fix this self-organized architecture in place, followed by removal of the imprinted template from the polymeric network, which thereby leaves behind binding sites stereochemically complementary to the template. For the preparation of catalytic MIPs, the templates usually used are the transition state or its analogue (transition state analogue; TSA), generating active sites for the activation of substrate.^[10,11] The arrangement of the binding sites constitutes an induced molecular memory, which makes the prepared polymer capable of recognizing the imprint species and of catalyzing the specific substrate of TSA. Thus, host-guest interactions within the molecular imprinting system are usually comparable to typical biosystems, such as antibody–antigen, receptor–ligand and enzyme–substrate.

Smart imprinting systems are at the forefront of MIP technology, exhibiting stimulus-responsive recognition and/or catalytic ability. One typical example is poly(*N*-isopropylacrylamide) (PNIPAm)-based MIPs, which demonstrate thermosensitive molecular recognition and/or catalytic activity resulting from the thermal phase transition of PNIPAm.^[12,13] The hydrophobicity of PNIPAm increases with increasing temperatures. Thus, at higher temperatures, the PNIPAm networks shrink in water and the accessibility of analyte to the imprinted networks decreases, leading to lower molecular recognition and catalytic activity, i.e., the PNIPAm-based MIPs demonstrate negative thermal responsiveness. However, such negatively thermosensitive molecular recognition and/or catalytic activity generally does not have a high potential for practical application, simply because of the low activity and responsive kinetics at low temperatures. Furthermore, it is difficult to identify the polymer's hydrophilic/hydrophobic properties during the reaction. Thus, an alternative approach is advocated to create a new generation of smart MIPs.

1. Introduction

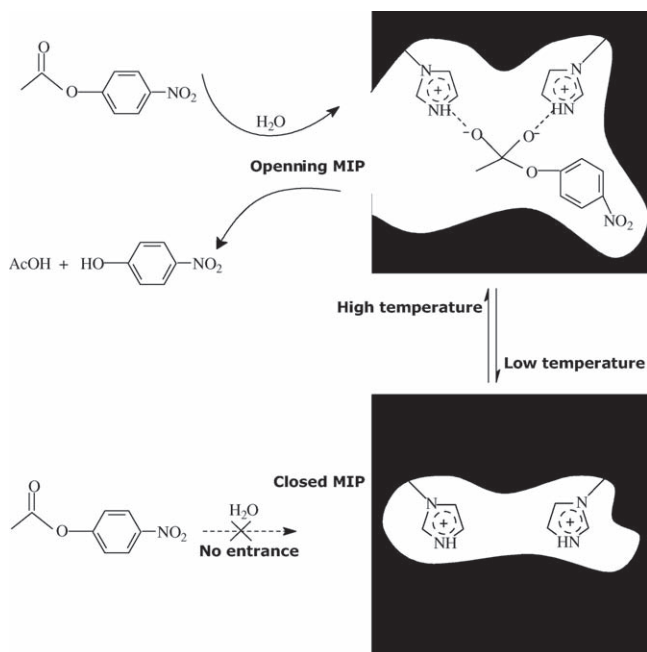
Molecular imprinting has attracted considerable attention in recent years because of its importance in the preparation of antibody-like polymers.^[1–3] This 'from-key-to-lock' technology generates molecularly imprinted polymers (MIP) capable of

Dr. S. Li
Key Laboratory of Pesticide & Chemical Biology of Ministry of Education
College of Chemistry
Central China Normal University
Wuhan 430079, China

Dr. S. Li, Dr. Y. Ge, Prof. A. P. F. Turner
Cranfield Health
Vincent Building
Cranfield University
Cranfield, Bedfordshire, MK43 0AL, UK
E-mails: y.ge@cranfield.ac.uk; a.p.turner@cranfield.ac.uk

Prof. A. P. F. Turner
Biosensors & Bioelectronics Centre
IFM, Linköping University
SE-58183, Linköping, Sweden
E-mail: anthony.turner@liu.se

DOI: 10.1002/adfm.201001906



Scheme 1. Proposed mechanism for the positively thermosensitive catalysis by MIP-R.

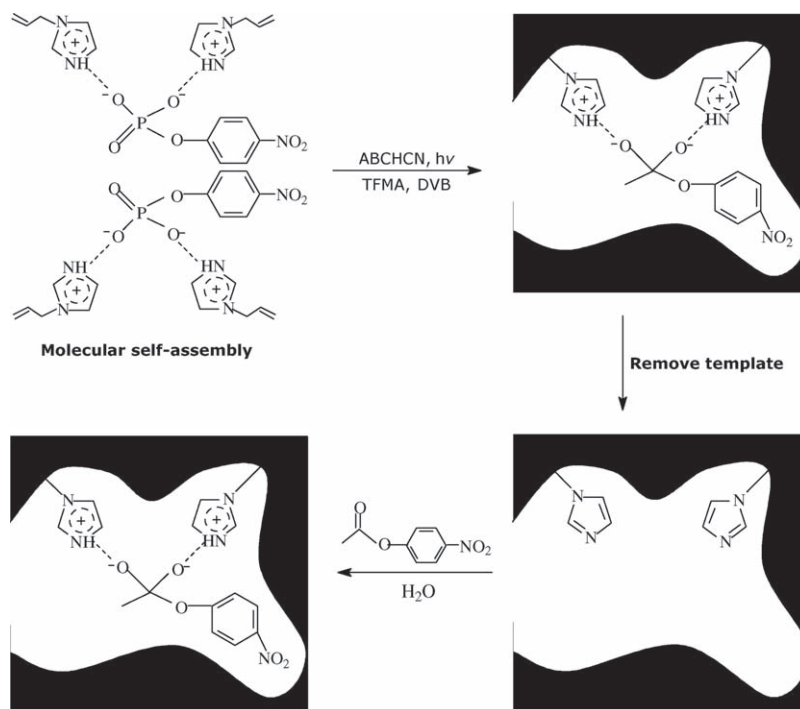
To the best of our knowledge, this paper represents the first report of a catalytic and positively thermosensitive molecularly imprinted polymer (i.e., MIP-R) (**Scheme 1**). In order to prepare the MIP-R, the hydrolysis of 4-nitrophenyl acetate (NPA) was selected as a model reaction, as it is compatible with water and has a well-proven TSA (i.e., 4-nitrophenyl phosphate; NPP) (cf. **Scheme 2**).^[14] NPP was imprinted in a unique polymeric matrix made up of poly(2-trifluoromethylacrylic acid) (PTFMA) and poly(1-vinylimidazole) (PVI),^[15] which contains hydrolytically active sites in the form of imidazole groups. The interpolymer complexation and dissociation^[16,17] between PVI and PTFMA in response to a temperature change can control the accessibility of analyte to the active binding sites (**Scheme 1**). At relatively low temperatures, the interpolymer complexation between PVI and PTFMA blocked access to the active sites of PVI and caused shrinking of the polymer, thus inhibiting catalysis. In contrast, at relatively high temperatures, the dissociation of the interpolymer complexes facilitated access to the active sites of PVI and inflated the polymer, enabling the catalysis. In this way, positively thermosensitive catalysis could be achieved by using this unique “smart” imprinted polymer. For comparison, three control polymers, namely MIP, NIP, and NIP-R were also prepared under comparable conditions (see Experimental Section). MIP and NIP were the conventional imprinted and non-imprinted polymers, respectively, with the same composition as MIP-R (the molecularly imprinted responsive polymer) but

without PTFMA in their polymeric networks. NIP-R was the thermosensitive non-imprinted polymer that contained the same amount of PTFMA as MIP-R. In order to investigate the catalytic specificity, 4-nitrophenyl butyrate (NPB), the structural analogue of NPA, was selected as the control. The purpose of this study is to realize the intriguing concept of developing a catalytic and positively thermosensitive molecularly imprinted polymer.

2. Results and Discussion

2.1. Rationally Optimized Interactions Within Imprinted Polymers

It is well known that molecular self-assembly plays an important role in the pre-determination of the properties of an imprinted polymer. An excessive amount of monomer over the template would cause spatial and steric mismatch due to the excessive binding sites that distribute randomly throughout the polymer. Conversely, an underestimated amount of monomer will deliver a polymer with an insufficient quantity of active binding sites. Thus, only stoichiometric amounts of monomer can result in an optimized imprinted polymer.^[18] In order to ensure a complete blockage and release of these active binding sites (i.e., imidazole groups), the final polymer should also contain stoichiometric TFMA–VI interaction. Too low or too high an amount of TFMA would not result in the complete complexation and dissociation of PTFMA and PVI. Thus, dual stoichiometric interactions between the template, monomer, and TFMA are needed to achieve an optimal smart imprinted polymer. With these points



Scheme 2. Schematic representation of the preparation of MIP-R.

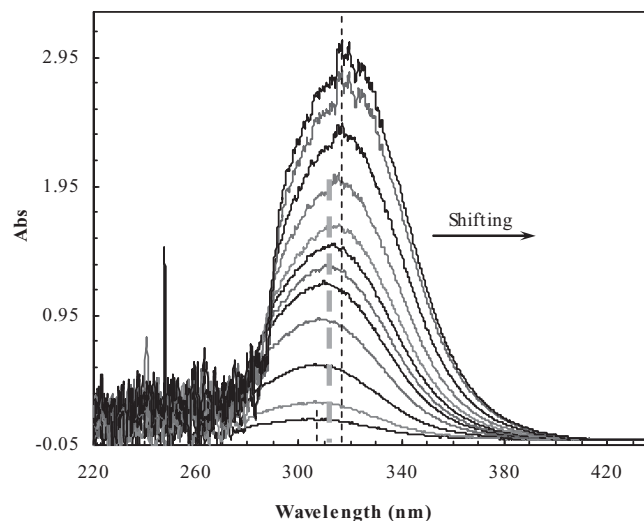


Figure 1. The change of UV spectra as a function of VI/NPP molar ratio, (In which, NPP (7.5 mmol L^{-1} ; $10 \text{ }\mu\text{L}$ /titration) was titrated into VI (0.5 mmol L^{-1} ; 2.5 mL)

in hand, **Figures 1** and **2** present the UV spectra used to monitor these interactions as functions of the VI/NPP and TFMA/VI ratios. Using a proportional composition as the control and initial baseline (**Table 1**), NPP and TFMA were titrated into VI, respectively. Both titrations caused shifts in the UV spectra. Both the shifts achieved maximal values when the titrated NPP and TFMA reached a critical amount (corresponding to the 1.67 mol/mol VI/NPP ratio and 1.18 mol/mol TFMA/VI ratio). Beyond the critical values, no further shift in the UV spectra was observed except for increasing absorbency. It is therefore clear that the VI–NPP and VI–TFMA interactions are saturated by the stoichiometric titrations. Based on the original NPP (0.5 mmol), 0.835 mmol VI and 0.985 mmol TFMA were therefore used to prepare the thermosensitive MIP-R and its control polymers. In this context, further studies were performed as shown below.

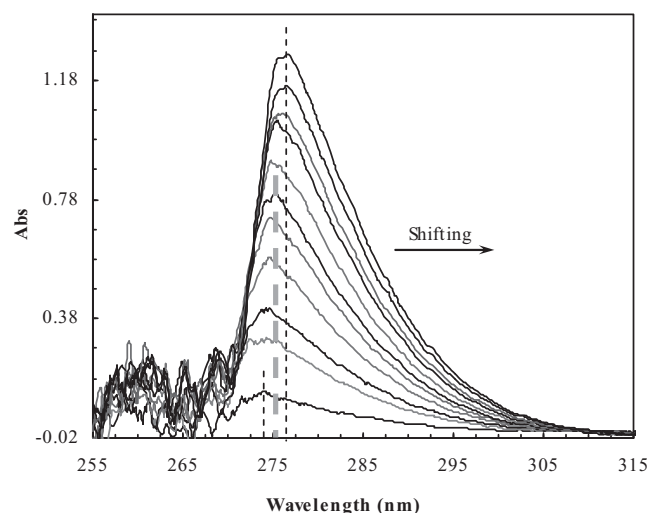


Figure 2. The change of UV spectra as a function of TFMA/VI molar ratio, (In which, TFMA (0.2 mol L^{-1} ; $50 \text{ }\mu\text{L}$ /titration) was titrated into VI (0.03 mol L^{-1} ; 2.5 mL)

Table 1. Synthesis composition of imprinted and non-imprinted polymers.

Composition	MIP-S	MIP	NIP-R	NIP
NPP	0.11g (0.5 mmol)	0.11g (0.5 mmol)	/	/
VI	78.6mg (0.835 mmol)	78.6mg (0.835 mmol)	78.6mg (0.835 mmol)	78.6mg (0.835 mmol)
TFMA	137.9mg (0.985 mmol)	/	137.9mg (0.985 mmol)	/
DVB	1.42 mL (8.0 mmol)	1.42 mL (8.0 mmol)	1.42 mL (8.0 mmol)	1.42 mL (8.0 mmol)
ABCHCN	0.6 g (2.46 mmol)	0.6 g (2.46 mmol)	0.6 g (2.46 mmol)	0.6 g (2.46 mmol)

2.2. FTIR Spectra and SEM Morphology

In order to ascertain the imprinting behavior, FTIR spectra of the prepared MIP-R, NPP, and the MIP-R precursor (i.e., the MIP-R system where the imprinted NPP had not yet been removed from the polymer matrix) were obtained (**Figure 3**). Three characteristic peaks ($3200\text{--}3700$, $2800\text{--}3200$, $\sim 1750 \text{ cm}^{-1}$) and one broad fingerprint band ($1000\text{--}1600 \text{ cm}^{-1}$) appeared in the spectra of both MIP-R and its precursor. These characteristic peaks can be attributed to the stretching vibration of O–H/N–H, C–H, and C=O.^[19,20] The fingerprint band may arise from C–N and C–C bonds and their rotation. For comparison, we also included the spectra of the control polymers in **Figure 3**. The MIP-R precursor, MIP-R and NIP-R demonstrated an absorption peak at $\sim 1750 \text{ cm}^{-1}$, which is closely associated with the stretching vibration of C=O in PTFMA, but MIP and NIP did not. This result suggests that these thermosensitive polymers did have PTFMA in their polymeric networks. As further noted, the MIP-R precursor showed the characteristic peaks of both NIP-R and NPP, implying the complicated composition of the MIP-R precursor. After washing, the spectrum of the MIP-R precursor became comparable to NIP-R. This result strongly suggests that the molecular imprinting of NPP did occur during the preparation, as expected.

Figure 4 shows the SEM images of these synthetic polymers. These polymers appeared spherical in morphology and were about $1.5\text{--}2 \text{ }\mu\text{m}$ in diameter. Compared with MIP and NIP, both MIP-R and NIP-R had somewhat uneven surfaces. This observation probably results from the PTFMA contained, which is present in the polymeric networks and therefore partially affected the surface of both MIP-R and NIP-R. Thus, the successful preparation of both thermosensitive and traditional polymers provides a convenient framework for straightforward and comparative studies.

2.3. Specific Interaction Between Polymers and Analyte

Figure 5 displays the temperature-programmed desorption (TPD) profiles, with the purpose of characterizing the interaction between these prepared polymers and analyte.^[21,22] MIP-R and MIP both demonstrated significant separation abilities

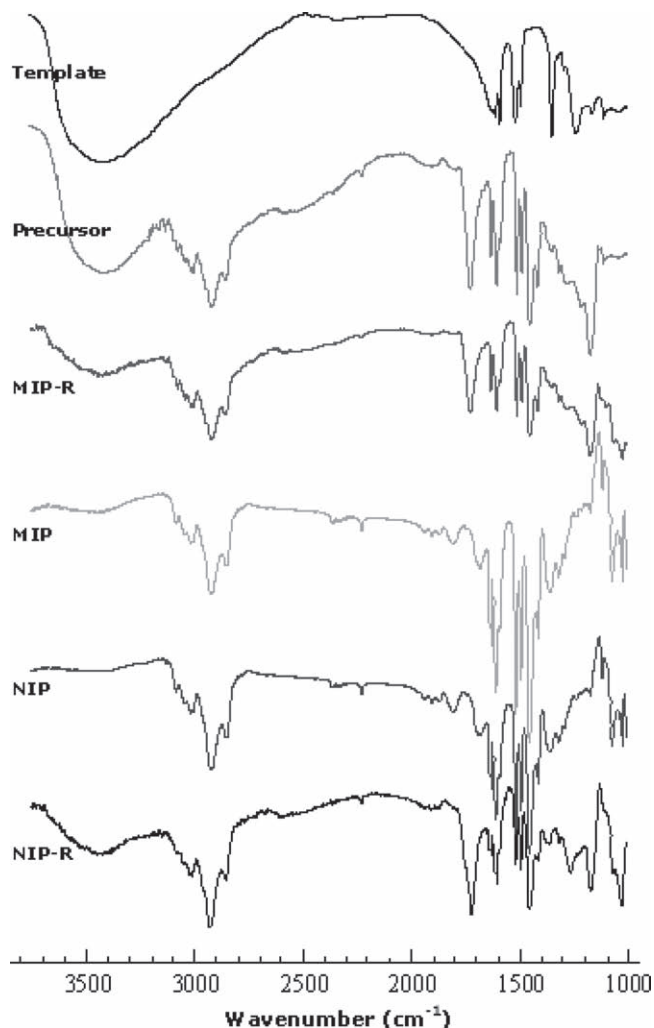


Figure 3. FTIR spectra of the prepared polymers.

for NPA and NPB, but NIP and NIP-R did not. This result indicates that the interaction between both the imprinted polymers (i.e., MIP-R and MIP) and NPA is highly specific and capable of separation of NPA and NPB. In conjunction with the characterization of molecular imprinting, this result reflects again a consequence of the NPA-specific imprint. Since MIP-R and MIP both contained imprinted structures in their polymeric networks, such separation ability is to be expected.

2.4. Thermosensitive Interaction Behavior

Dynamic light scattering (DLS) was used to evaluate the inter-polymer interaction within the prepared polymers.^[23,24] In order to allow equilibrium reaching, all samples were kept at each tested temperature for 10 min before measurement of the hydrodynamic size of particles. Through a comparison between the thermosensitive and non-thermosensitive polymers, the relative change of the hydrodynamic particle size (R_c) reflected the contribution of the PVI-PTFMA interaction. As shown

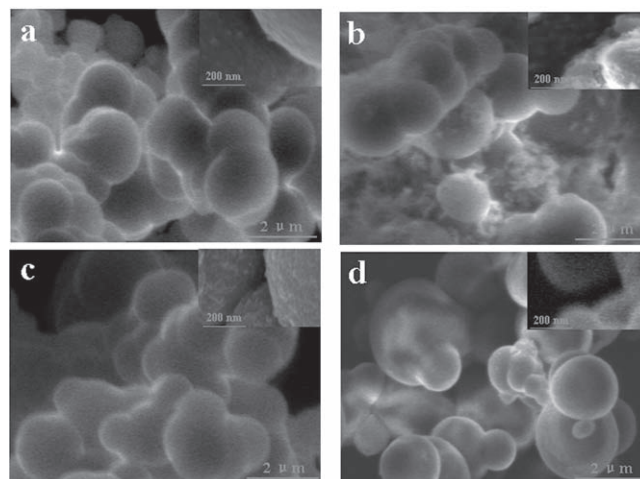


Figure 4. SEM images of the prepared polymers (a: NIP; b: NIP-R; c: MIP; d: MIP-R)

in Figure 6, MIP-R and NIP-R both demonstrated significant dependencies on temperature in comparison with the conventional MIP and NIP, as expected. The R_c of MIP-R and NIP-R both increased with increased temperature. A dramatic increase

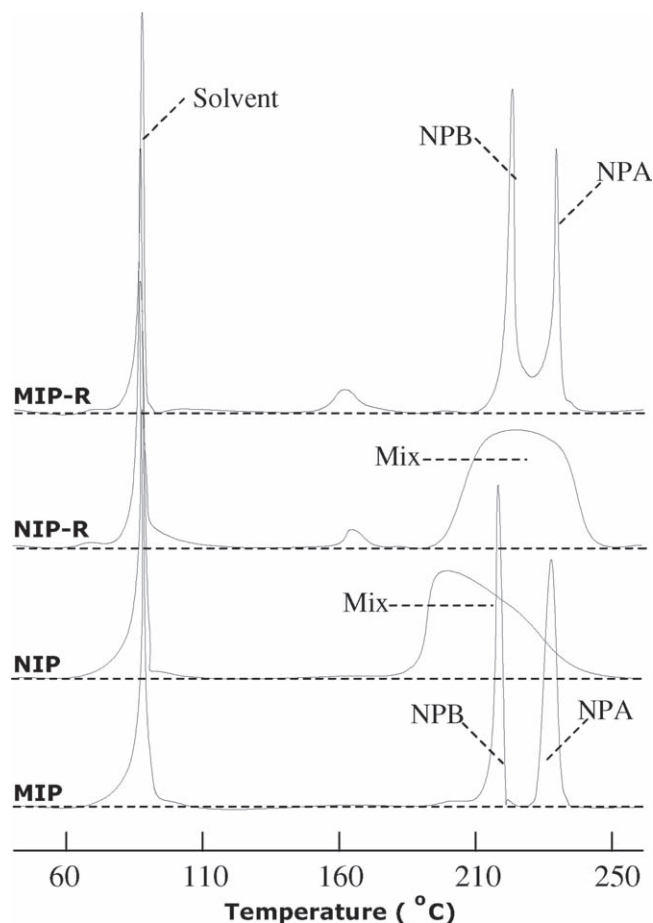


Figure 5. TPD profiles of the prepared polymers.

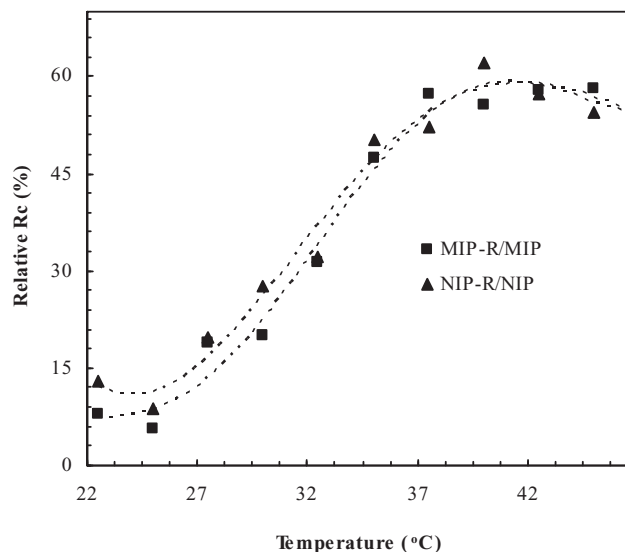


Figure 6. DLS curves of the prepared polymers.

in the R_c of MIP-R and NIP-R occurred at circa 27–35 °C. Below this temperature region, MIP-R and NIP-R exhibited a relatively small R_c ; however, above this temperature region, they demonstrated a dramatic increase. As previously explained, this may be attributed to the unique interpolymer interaction between PVI and PTFMA. The small R_c at relatively low temperatures may be due to the interpolymer complexation between PVI and PTFMA, which inhibited access of water to the polymer interior and thereby restricted the polymeric networks (Scheme 1). The increased R_c at relatively high temperatures can be attributed to the dissociation of the interpolymer complexes, which facilitated access of water to the polymer interior and thus relaxed the polymeric networks.

2.5. Switched Catalysis

Figure 7 presents the catalysis of the prepared polymers. In view of the occurrence of self-hydrolysis during the catalytic process, which can affect the true catalytic activity of test polymers, the hydrolysis of analyte without any polymer was deducted from the overall activity of these polymers. For comparison, herein two representative temperatures, i.e., 40 and 20 °C (either higher or lower than the thermosensitive region of MIP-R and NIP-R, i.e., 27–35 °C) were selected for a contrastive study. It was observed that MIP-R at 40 °C was comparable to MIP and demonstrated significant catalysis for the hydrolysis of NPA. However, MIP-R at 20 °C more resembled NIP-R and NIP, which demonstrated limited catalytic ability for the hydrolysis of NPA. MIP-R apparently showed a thermo-switchable catalysis mechanism. Clearly, this result can be attributed to the unique interpolymer interaction within MIP-R. The complexation and dissociation between PVI and PTFMA regulated the accessibility of reactants to the imprinted networks, thereby inducing the switched catalysis.

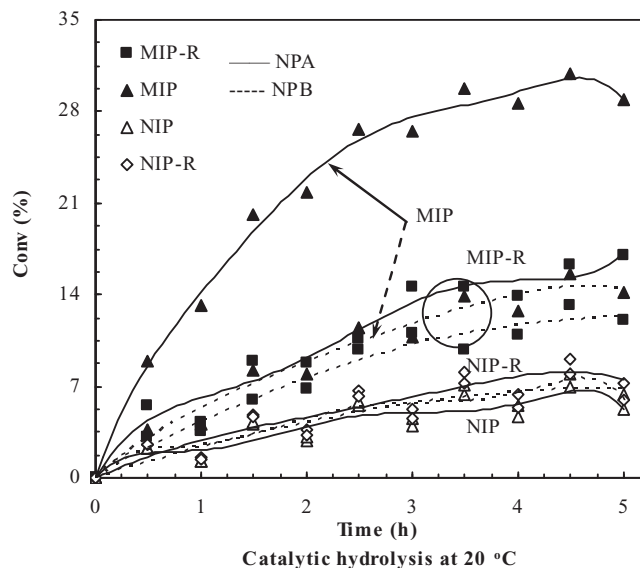
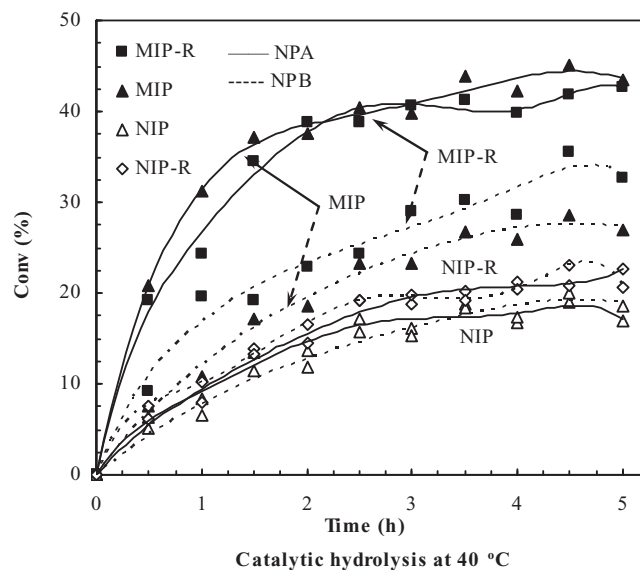


Figure 7. Catalysis of the prepared polymers at 20 and 40 °C.

2.6. Switchable Binding Behavior

It is known that the potential to reduce/oxidize a binding molecule depends on the binding constant. A larger binding constant requires more energy to overcome the binding force, thereby causing a larger redox potential. Thus, dynamic desorbing cyclic voltammetry (DCV) can provide valuable information about the binding behavior of the prepared polymers with their template.^[25] As shown in Figure 8, the template NPP that was bound to MIP-R at 20 °C exhibited a reduction peak at –699.2 mV (Figure 8a). In contrast, at 40 °C, this reduction peak shifted to a lower potential (i.e., –729.8 mV) (Figure 8b). MIP-R demonstrated a stronger interaction with the template at 40 °C than at 20 °C.

For comparison, Figure 8c–h also includes the reduction potentials of NPP from these control polymers. The

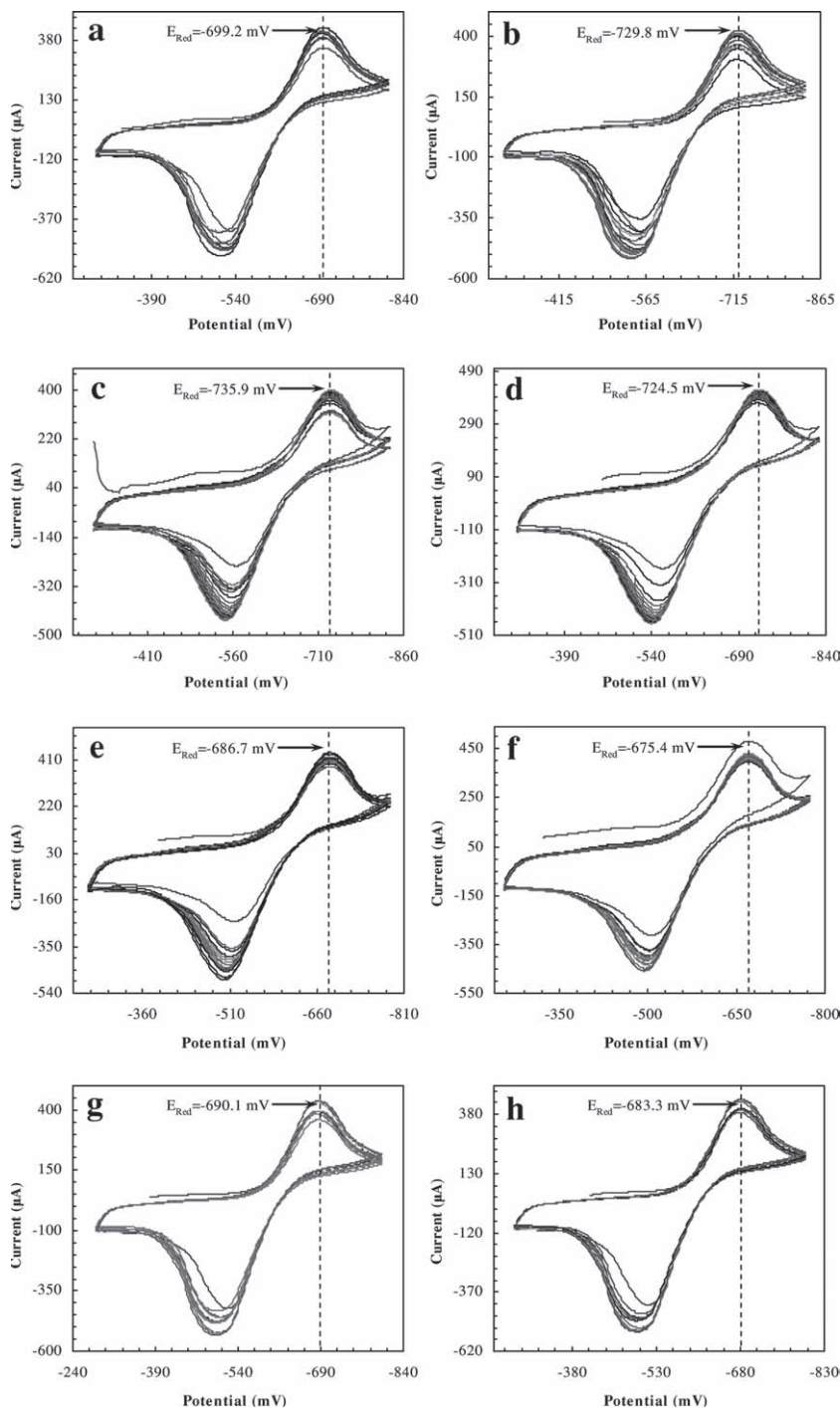


Figure 8. DCV profiles of the template NPP from the prepared polymers. a) MIP-R at 20 °C; b) MIP-R at 40 °C; c) MIP at 20 °C; d) MIP at 40 °C; e) NIP at 20 °C; f) NIP at 40 °C; g) NIP-R at 20 °C; h) NIP-R at 40 °C

reduction potential of the NPP that was bound to MIP-R at 40 °C was nearly comparable to that was from MIP (−729.8 vs. −724.5 mV). The reduction potential of the NPP that was bound to MIP-R at 20 °C became as low as that from NIP-R (−699.2 vs. −690.1 mV). This result strongly suggests that MIP-R did provide a thermo-switchable interaction with the template. Again, this

result can be attributed to the unique thermo-sensitive mechanism of the MIP-R networks. The thermo-sensitive interaction between MIP-R and its analyte regulated the access to molecularly imprinted networks, thereby making the switched binding feasible.

3. Conclusions

The concept of a catalytic, positively thermo-sensitive molecularly imprinted polymer has been demonstrated for the first time. This imprinted polymer was composed of a TSA-imprinted matrix that demonstrated a thermo-sensitive complexation and dissociation between poly(1-vinylimidazole) and poly(2-trifluoromethylacrylic acid). At a relatively low temperature (such as 20 °C), the polymer did not demonstrate significant catalysis; however, at higher temperatures it presented significant catalysis. These results indicate that a catalytic, positively thermo-sensitive molecularly imprinted polymer can be fabricated using this novel design.

4. Experimental Section

Preparation of Imprinted Polymers: Chemicals were of analytic grade and used as received from Sigma-Aldrich, except for 1-vinylimidazole (VI) and divinylbenzene (DVB), which were washed with 5 wt% sodium hydroxide solution prior to use. The preparation of these mentioned polymers, as previously discussed, was based on the optimized template/monomer and monomer/TFMA ratios (Table 1). The template–monomer complex was first formed by adding a stoichiometric amount of VI into NPP. Subsequently, the complex, DVB, 1,1'-azobis(cyclohexane-1-carbonitrile) (ABCHCN) and a stoichiometric amount of TFMA were dissolved in the mixture of acetonitrile/dimethylsulfoxide (each 5.0 mL) to form a homogeneous system. After being deoxygenated with sonication and nitrogen, the mixed system was irradiated by ultraviolet light (365 nm) overnight. The resulting polymers were crushed roughly and extracted with ethanol containing 20% acetic acid using a Soxhlet apparatus for 24 h. The products were profusely washed with ethanol and dried at room temperature.

SEM and FTIR Analysis: The morphology of these prepared polymers was studied using a scanning electron microscopy (FEI XL30 SFEG) (FEI-Philips, USA). The acceleration voltage used was 10.0 kV. The infrared spectra were recorded using an Avatar 370 FT-IR apparatus (ThermoNicolet, USA).

TPD: Using a device comprising of a gas chromatograph (TCD) and a data processing system, the test polymer (10 mg) were placed into an online U-shaped quartz tube (4 mm I.D.). After 10 µL of analyte (0.01 µmol mL^{−1} in acetonitrile) was pre-adsorbed by these polymers, the U-shaped tube was heated under a nitrogen flow (40 mL min^{−1}, 0.23 MPa) at 10 °C min^{−1} from room temperature to the temperature where the analyte desorbed. The desorbing signal was recorded by the data processing system.

DLS: The DLS analysis was carried out at a scattering angle of 90° using a goniometer equipped with a self-rotation unit and a He–Ne laser (Mastersizer-X) (Malvern, UK). All samples were kept at each tested temperature for 10 min in water (containing circa 5% acetonitrile), in order to reach equilibrium. The relative change of hydrodynamic particle size (R) reflecting the contribution of the PVI–PTFMA interaction was calculated as follows:

$$R_c = \left[\left(\frac{R_w - R_d}{R_d} \right)_T - \left(\frac{R_w - R_d}{R_d} \right)_{NT} \right] \times 100\%$$

Herein, T indicates the thermosensitive polymers and NT represents the corresponding non-thermosensitive polymers. R_w is the particle size of polymers in water, while R_d is the corresponding that of dried particles

Catalysis Test: The catalytic properties of these polymers were evaluated in a batch format using a thermostated apparatus (pH 7.0 PBS containing circa 5% acetonitrile).^[26] The initial concentration of analyte (NPA or NPB) was 0.01 $\mu\text{mol mL}^{-1}$ (totally 10 mL). The solid content of the test polymer was 2.5 mg mL^{-1} in each test. The 4-nitrophenolate produced was spectrophotometrically monitored at 400 nm. The activity of these polymers was recorded based on the average value of identical triple runs. The self-hydrolysis of analyte without polymer was also performed under comparable conditions and was finally deducted from the corresponding overall activity.

DCV: Using an electrochemical workstation equipped with a three-electrode configuration (Pt-working and counter electrodes; Ag/Ag⁺-reference.) (LK9806) (Lanlike, China), the test polymer (10 mg) that pre-absorbed circa 1 μmol template was placed into a cuvette encircled by a diffusion-eliminated sonication apparatus (supporting electrolyte: 0.01 mmol mL^{-1} KCl; 10 mL). The transiently desorbed template was rapidly scanned by the workstation using up to 20 cycles until a stable dynamic cyclic voltammogram was achieved (scanning range, from –800 to –200 mV; scanning rate, 25 mV s^{-1}).

Acknowledgements

The authors would like to thank the Research Directorate-General of European Commission for supporting this work under the framework of Marie Curie Actions (No. PIIF-GA-2009–236799). Thanks should also be expressed to the National Science Foundation of China (No. 21073068).

Received: September 11, 2010

Published online: February 25, 2011

- [1] A. Pietrzyk, S. Suriyanarayanan, W. Kutner, R. Chitta, F. D'Souza, *Anal. Chem.* **2009**, *81*, 2633.
- [2] D. Lakshmi, A. Bossi, M. J. Whitcombe, I. Chianella, S. A. Fowler, S. Subrahmanyam, E. V. Piletska, S. A. Piletsky, *Anal. Chem.* **2009**, *81*, 3576.
- [3] Y. Zhang, R. Liu, Y. Hu, G. Li, *Anal. Chem.* **2009**, *81*, 967.
- [4] C. Zhai, Q. Lu, X. Chen, Y. Peng, L. Chen, S. Du, *J. Chromatogr. A* **2009**, *1216*, 2254.
- [5] J. Lejeune, D. A. Spivak, *Biosens. Bioelectr.* **2009**, *25*, 604.
- [6] M. Saraji, H. Yousefi, *J. Hazard. Mater.* **2009**, *167*, 1152.
- [7] Y. Lv, Z. Lin, T. Tan, W. Feng, P. Qin, C. Li, *Sens. Actuators B* **2008**, *133*, 15.
- [8] W. Li, S. Li, *Adv. Polym. Sci.* **2007**, *206*, 191.
- [9] J. Lee, S. Bernard, X. C. Liu, *React. Funct. Polym.* **2009**, *69*, 650.
- [10] P. Pasetto, K. Flavin, M. Resmini, *Biosens. Bioelectr.* **2009**, *25*, 572.
- [11] K. Tong, S. Xiao, S. Li, J. Huang, *J. Inorg. Organomet. Polym.* **2008**, *18*, 426.
- [12] S. Li, S. Pilla, S. Gong, *J. Polym. Sci. A* **2009**, *47*, 2352.
- [13] H. Tokuyama, S. Naohara, M. Fujioka, S. Sakohara, *React. Funct. Polym.* **2008**, *68*, 182.
- [14] D. Zhang, S. Li, W. Li, Y. Chen, *Catal. Lett.* **2007**, *115*, 169.
- [15] Y. Kawanami, T. Yunoki, A. Nakamura, K. Fujii, K. Umano, H. Yamauchi, K. Masuda, *J. Mol. Catal. A* **1999**, *145*, 107.
- [16] X. C. Xiao, L. Y. Chu, W. M. Chen, S. Wang, Y. Li, *Adv. Funct. Mater.* **2003**, *13*, 847.
- [17] V. V. Khutoryanskiy, Z. S. Nurkeeva, G. A. Mun, A. V. Dubolozov, *J. Appl. Polym. Sci.* **2004**, *93*, 1946.
- [18] B. C. G. Karlsson, J. O'Mahony, J. G. Karlsson, H. Bengtsson, L. A. Eriksson, I. Nicholls, *J. Am. Chem. Soc.* **2009**, *131*, 13297.
- [19] W. Wang, X. Tian, Y. Feng, B. Cao, W. Yang, L. Zhang, *Ind. Eng. Chem. Res.* **2010**, *49*, 1684.
- [20] M. Recillas, L. L. Silva, C. Peniche, F. M. Goycoolea, M. Rinaudo, W. M. Arguelles-Monal, *Biomacromolecules* **2009**, *10*, 1633.
- [21] S. Li, S. Gong, S. Adv. Funct. Mater. **2009**, *19*, 2601.
- [22] S. Li, C. Liao, W. Li, Y. Chen, X. Hao, *Macromol. Biosci.* **2007**, *7*, 1112.
- [23] Y. Lu, Y. Mei, M. Drechsler, M. Ballauff, *Angew. Chem. Int. Ed.* **2006**, *45*, 813.
- [24] S. Li, X. Huang, M. Zheng, W. Li, *Anal. Bioanal. Chem.* **2008**, *392*, 177.
- [25] S. Li, S. Gong, *J. Phys. Chem. B* **2009**, *113*, 16501.
- [26] S. Li, K. Tong, D. Zhang, X. Huang, *J. Inorg. Organomet. Polym.* **2008**, *18*, 264.